Free Radical Biology and Medicine 226 (2025) 251–265

Contents lists available at ScienceDirect

Free Radical Biology and Medicine

journal homepage: www.elsevier.com/locate/freeradbiomed

Itaconic acid ameliorates necrotizing enterocolitis through the TFEB-mediated autophagy-lysosomal pathway

Baozhu Chen [a,b,1], Yufeng Liu [c,1], Shunchang Luo [a,b,1], Jialiang Zhou [d], Yijia Wang [a,b], Qiuming He [e], Guiying Zhuang [f], Hu Hao [a,b,*], Fei Ma [g,**], Xin Xiao [a,b,***], Sitao Li [a,b,h,****]

[a] Department of Pediatrics, The Sixth Affiliated Hospital, Sun Yat-sen University, Guangzhou, 510655, China
[b] Biomedical Innovation Center, The Sixth Affiliated Hospital, Sun Yat-sen University, 510655, China
[c] Center for Medical Research on Innovation and Translation, Guangzhou First People's Hospital, The Second Affiliated Hospital of South China University of Technology, Guangzhou, Guangdong 510000, China
[d] Department of Neonatal Surgery, Guangdong Women and Children Hospital, Guangzhou, 510010, China
[e] Department of Surgical Neonatal Intensive Care Unit, Guangzhou Women and Children's Medical Center, Guangzhou Medical University, Guangzhou 510623, China
[f] The Maternal and Children Health Care Hospital (Huzhong Hospital) of Huadu, No. 17 Industrial Avenue, Huadu District, Guangzhou, Guangdong, 510800, China
[g] Maternal & Child Health Research Institute, Zhuhai Center for Maternal and Child Health Care, Zhuhai, 519001, China
[h] Department of Pediatrics, Xinyi People's Hospital, Maoming, 525300, China

ARTICLE INFO

Keywords:
Necrotizing enterocolitis
Itaconic acid
Autophagy-lysosomal pathway
Lysosomal dysfunction
TFEB

ABSTRACT

Excessive autophagy has been implicated in the pathogenesis of necrotizing enterocolitis (NEC), yet the molecular underpinnings of the autophagy-lysosomal pathway (ALP) in NEC are not well characterized. This study aimed to elucidate alterations within the ALP in NEC by employing RNA sequencing on intestinal tissues obtained from affected infants. Concurrently, we established animal and cellular models of NEC to assess the therapeutic efficacy of itaconic acid (ITA). Our results indicate that the ALP is significantly disrupted in NEC. Notably, ITA was found to modulate the ALP, enhancing autophagic flux and lysosomal function, which consequently alleviated NEC symptoms. Further analysis revealed that ITA's beneficial effects are mediated through the promotion of TFEB nuclear translocation, thereby augmenting the ALP. These findings suggest that targeting the ALP with ITA to modulate TFEB activity may represent a viable therapeutic approach for NEC.

1. Introduction

Necrotizing enterocolitis (NEC) is a devastating neonatal gastrointestinal condition that can progress rapidly from initial symptoms to severe illness and death within 24–48 h of onset [1,2]. Clinical diagnosis of NEC is confirmed through the identification of pneumatosis intestinalis, portal venous gas, or by direct visualization of the bowel during surgery [1]. Currently, pharmacological options are limited, with surgical treatment remaining the predominant therapeutic approach [1,3–5]. However, the postoperative period is fraught with complications such as intestinal strictures, adhesions, cholestasis, short bowel syndrome, dysplasia, and neurodevelopmental delays [2,6]. There is an urgent need to better understand the pathogenic mechanisms of NEC to develop more potent treatments.

Emerging evidence suggests that abnormal autophagy is associated with bowel inflammation, as seen in NEC, which is characterized by

Abbreviations: ACOD1, aconitate decarboxylase 1 Gene; ALP, autophagy-lysosome pathway; CQ, chloroquine; CTSD, cathepsin D; DMEM, dulbecco's modified eagle medium; GC-MS, gas chromatography-mass spectrometry; GSEA, gene set enrichment analysis; H&E, hematoxylin and eosin; HIEC, human intestinal epithelioid cell; IPA, Ingenuity Pathway Analysis; IRG1, immune responsive gene 1; ITA, itaconic acid; NEC, necrotizing enterocolitis; TCA, tricarboxylic acid cycle; TEM, transmission electron microscopy; TFEB, transcription factor EB; VAMP8, vesicle-associated membrane protein 8.

* Corresponding authors. the Sixth Affiliated Hospital, Sun Yat-sen University, No. 26, Yuancun Erheng Road, Guangzhou, 510655, China.
** Corresponding author. Zhuhai Center for Maternal and Child Health Care, No.3366 Nanqin Road, Nanping, Xiangzhou District, Zhuhai, 519001, China.
*** Corresponding authors. the Sixth Affiliated Hospital, Sun Yat-sen University, No. 26, Yuancun Erheng Road, Guangzhou, 510655, China.
**** Corresponding author. The Sixth Affiliated Hospital, Sun Yat-sen University, No. 26, Yuancun Erheng Road, Guangzhou, 510655, China.
E-mail addresses: haohu@mail.sysu.edu.cn (H. Hao), mafei5@mail3.sysu.edu.cn (F. Ma), xiaoxin2@mail.sysu.edu.cn (X. Xiao), lisit@mail.sysu.edu.cn (S. Li).
[1] These authors contributed equally to this work.

https://doi.org/10.1016/j.freeradbiomed.2024.11.035
Received 4 September 2024; Received in revised form 9 November 2024; Accepted 18 November 2024
Available online 19 November 2024

Table 1
Clinical Characteristics of NEC and non-NEC patients.

Parameter	Sex (male/female)	GA (week)	BW (g)	5-min apgar	Intraoperative diagnosis	Bell stage
Control-1	Male	37^{+2}	2600	10	Intestinal atresia	
Control-2	Female	38^{+5}	2810	10	Intestinal atresia	
Control-3	Male	39^{+4}	3400	10	Intestinal atresia	
NEC-1	Male	34^{+3}	2730	9	Necrotizing enterocolitis	III
NEC-2	Female	27^{+3}	1010	7	Necrotizing enterocolitis	III
NEC-3	female	26^{+6}	1150	7	Necrotizing enterocolitis	III

impaired mucosal healing [7]. Autophagy, an intracellular lysosome-dependent degradation process, is crucial for maintaining cellular homeostasis and is often referred to as the autophagy-lysosomal pathway (ALP) [8–10]. Lysosomes, organelles responsible for degradation, play a key role in autophagy by breaking down intracellular components [11]. Transcription factor EB (TFEB), a key transcriptional factor of the ALP [8], was originally identified as a modulator of lysosomal biogenesis and degradation [12]. Several diseases have been linked to lysosomal dysfunction and alterations in autophagy [11, 13–15]. For instance, NEC induction leads to excessive autophagy and lysosomal overload, resulting in lysosomal membrane permeabilization and rupture, ultimately causing cell death [16].

Autophagy is intricately linked to cellular metabolism [11]. Metabolomic studies of Ras-expressing cancer cells have demonstrated that autophagy is essential for maintaining tricarboxylic acid (TCA) cycle metabolites [17]. Notably, citrate, aconitate, and isocitrate, all mitochondrially formed, are downregulated, suggesting that autophagy significantly contributes to TCA metabolites. Itaconic acid (ITA), produced via the TCA cycle by the decarboxylation of cis-aconitic acid by ACOD1 (also known as immune response gene 1 [IRG1]) [18,19], connects metabolism, oxidative stress, immune response and inflammation. ITA has been shown to modify Cys212 of TFEB, disrupt TFEB phosphorylation, and induce TFEB nuclear translocation, promoting the ALP and thereby ameliorating inflammation [20]. However, the role of ITA in the ALP during NEC is yet to be determined.

Gas chromatography-mass spectrometry (GC-MS) analysis has revealed significant changes in serum metabolism in fed preterm infants, with a decrease in ITA, potentially serving as a predictive biomarker for NEC [21]. In this study, we demonstrate that the ALP is altered in neonatal intestines during NEC. Patients with NEC exhibit hyperactivated autophagy but a reduction in autophagic flux, seemingly due to ALP inhibition, which correlates with reduced TFEB expression levels. We found that ITA protected against NEC by upregulating TFEB, thereby improving the ALP. Our data position ITA as a promising therapeutic target for NEC.

2. Materials and methods

2.1. Intestinal tissue collection and storage

Small bowel samples from three neonates diagnosed with NEC intraoperatively at the Sixth Affiliated Hospital, Sun Yat-sen University, Guangzhou, China, were collected. Control samples were obtained from three neonates matched for gestational age, birth weight, and sex, who were admitted to the neonatal intensive care unit without NEC during the same period (Table 1). The study protocol, in accordance with the Declaration of Helsinki, was approved by the Ethics Committee of the Sixth Affiliated Hospital, Sun Yat-sen University (2022ZSLYEC-525), and written informed consent was obtained from each participant's parents.

Intestinal tissue samples were cut into sub-centimeter pieces, quickly frozen in liquid nitrogen, and stored at −80 °C for RNA and protein extraction for RNA sequencing (RNA-seq) and western blotting. For paraffin block preparation, tissues were fixed in 4 % formalin for 48 h, transferred to ethanol, and embedded in paraffin. For transmission electron microscopy (TEM), intestinal tissues were fixed in 2.5 % glutaraldehyde solution and dehydrated.

2.2. RNA-seq and data analysis

RNA-seq was conducted to identify differentially expressed genes between NEC lesions and normal tissues, and to associate signature genes with signaling pathways by grouping the NEC cohort into different subgroups based on median gene expression values with an adjusted $p < 0.05$. OE Biotech, Inc., Shanghai, China, provided technical support for sample preparation, library preparation, sequencing, and data analysis. Bioinformatic analysis was performed using OE Cloud tools at https://cloud.oebiotech.com/task/, and the volcano map and other graphics were constructed using R (https://www.r-project.org/) on the OE Cloud platform.

2.3. Mice and experimental design of the NEC model

C57BL/6 mice were supplied by the Experimental Animal Center of The Sixth Affiliated Hospital of Sun Yat-sen University (Guangzhou, China) and maintained in a specific pathogen-free facility. All animal procedures were approved by the Institutional Animal Care and Use Committee of the Sixth Affiliated Hospital, SunYat-sen University (protocol number: IACUC-2022082601). NEC was induced in 6- to 8-day-old mouse pups by gavage feeding (five times daily) with Similac Advance infant formula (Abbott Nutrition, Columbus, OH, USA) and Esbilac puppy milk replacer (PetAg, Hampshire, IL, USA) at a ratio of 2:1, containing enteric bacteria from a patient with surgically confirmed NEC (12.5 μL of original stool slurry in 1 mL of formula) [22–24]. Mice were simultaneously exposed to hypoxic conditions (5 % O2, 95 % N2) for 10 min twice a day for 4 days in a modular chamber. For prophylactic treatment with ITA (Cat. No. I29204; Sigma, St. Louis, MO, USA), mice were treated intraperitoneally (i.p.) at various concentrations of 10, 20, 40, 60 mg/kg b.w. in a total volume of 10 μL once a day for 4 days, beginning 1 day before the initiation of NEC model construction. For ITA treatment, mice were injected i.p. with 40 mg/kg b.w. in a total volume of 10 μL once daily for 4 days, starting at the end of the second day of NEC model construction. For chloroquine (CQ; Cat.#S6999; Selleck Chemicals, Shanghai, China) experiments, mice were injected i.p. with CQ at 30 mg/kg b.w. in a total volume of 10 μL once daily. Control mice remained with their dams for breastfeeding, while NEC-affected pups (NEC group) received intraperitoneal (i.p.) injections of the vehicle as a control for ITA administration. Additionally, there was a group treated with ITA combined with chloroquine (NEC + ITA + CQ group). Pups were tracked and weighed on days 1, 2, 3, and 4 of the study prior to the start of casting. Animals were euthanized at postnatal day 12 or earlier if they showed signs of NEC.

2.4. Tissue collection and injury evaluation

After abdominal incision, the gastrointestinal tract was carefully removed, and the small intestines were grossly evaluated. The terminal 3 cm (ileum) was immediately excised, and the terminal 1 cm of each sample was placed in buffered 10 % paraffin for hematoxylin and eosin (H&E) staining. The severity of mucosal injury was graded on a scale of 0–4 by two independent pathologists blinded to the H&E staining results. Tissues with histological scores ≥2 were considered to have NEC [25].

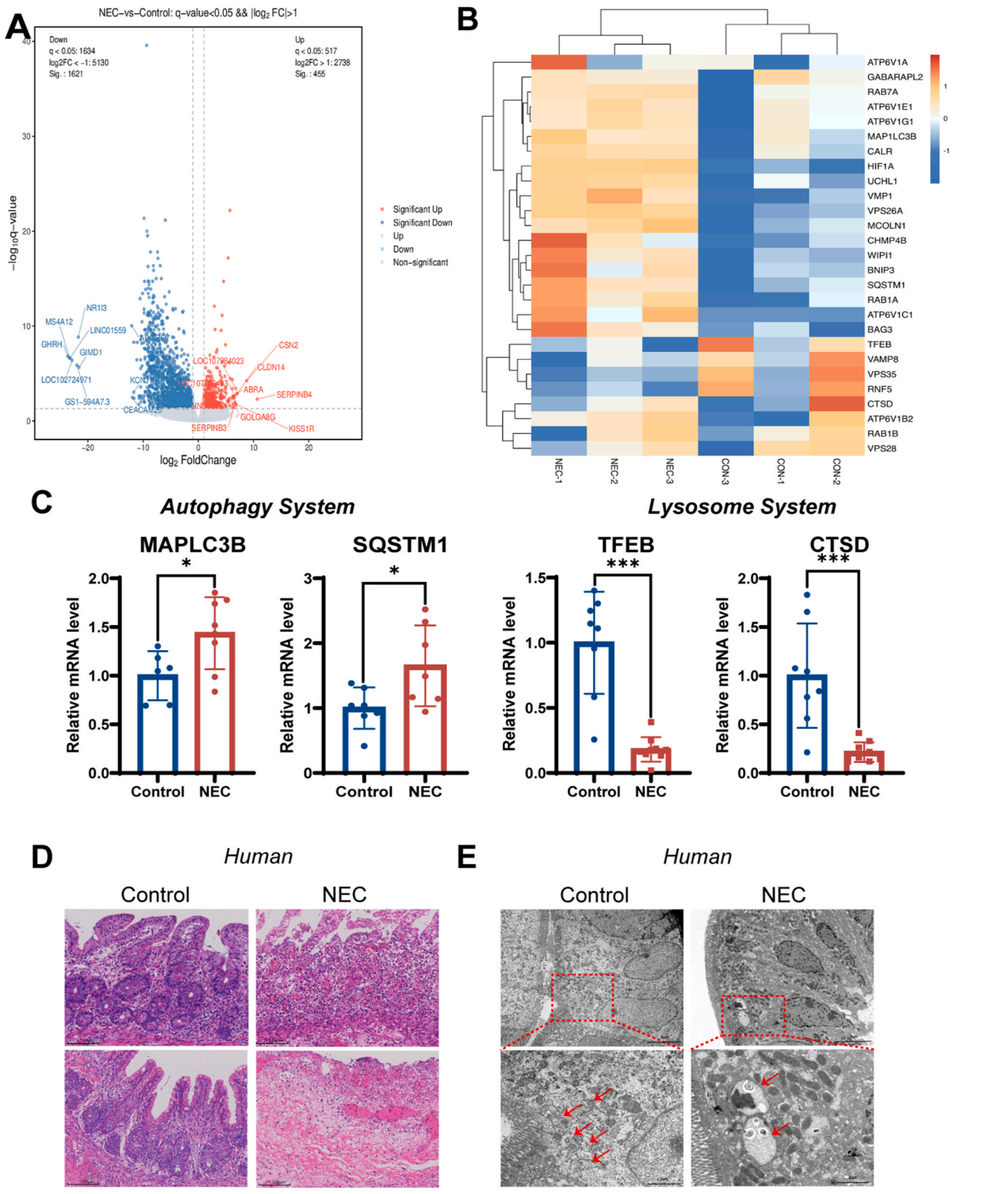

Fig. 1. Notable differences in the ALP are observed between the control and NEC groups.
(A) The volcano plot illustrates differentially expressed genes (DEGs) between the control and NEC groups. **(B)** RNA-Seq analysis of NEC infants (N = 3) presents a heatmap for 27 transcripts of autophagy-lysosomal-related genes, identified via Ingenuity Pathway Analysis (IPA). **(C)** Expression levels of autophagy-lysosomal pathway-related genes (*MAPLC3B, SQSTM1, TFEB,* and *CTSD*) were compared between the control and NEC groups using qRT-PCR, with data normalized to GAPDH. Data are depicted as the mean ± standard deviation (SD). *$p < 0.05$; ***$p < 0.001$. **(D)** Representative histology (H&E staining) of ileal sections from infants in the control and NEC groups is shown. Scale bar = 100 μm. **(E)** TEM images display autolysosomes within intestinal epithelial cells of NEC infants (top panel, scale bar = 5 μm; bottom panel, scale bar = 2 μm; red arrows indicate autolysosomes).

2.5. TEM

Small intestines were fixed with 2.5 % glutaraldehyde (Cat.#G1102-100 ML; Servicebio, Wuhan, China) and dehydrated. Ultrathin sections were mounted on copper grids and stained with uranyl acetate and lead citrate before imaging with an HT7800 TEM (HITACHI, Tokyo, Japan).

2.6. Cell culture

For in vitro experiments, the human intestinal epithelioid cell line 6 (HIEC6, Cat.# CTCC-004-0105, MeisenCTCC, Zhejiang China) was cultured in high-glucose-formulation Dulbecco's modified Eagle medium/Nutrient Mixture F-12 (DMEM/F12) supplemented with 10 % (v/v) fetal bovine serum and 10 ng/mL epidermal growth factor (EGF). The cells were then exposed to pro-inflammatory cytokines, including 10 ng/mL TNF-α and 5 ng/mL IL-1β, to induce inflammatory conditions for the I-HIEC6 group [26]. We assessed changes in cellular autophagic activity in response to the inflammatory incubation over a 48-h period. The concentration of CQ used to inhibit autophagy was 15 μM.

2.7. Cell counting kit-8 (CCK-8) assay

HIEC6 cells, showing robust growth, were plated at a density of 5 × 10^3 cells per well in 96-well plates. ITA treatment was performed at concentrations of 10, 20, 50, 100, and 200 μM for 24 h. Then, 10 μL of CCK-8 assay solution (Cat.#C0038; Life-iLab, Shanghai, China) was added to each well and incubated for 4 h. The absorbance of each well was measured at 450 nm using a Thermo FC microplate reader.

2.8. Western blotting analysis

Intestinal tissues and cultured cells were lysed with RIPA lysis buffer and centrifuged at 12,000 rpm for 15 min. The supernatant was collected, and protein concentration was determined using a bicinchoninic acid assay (BCA Protein Assay Kit, Cat. #P0010; Beyotime, Nanjing, China). Nuclear and cytoplasmic proteins were extracted using the Nuclear Protein and Cytoplasmic Protein Extraction Kit (Cat. #P0027, Beyotime, Nanjing, China). Proteins were resolved by electrophoresis using 12.5 % sodium dodecyl sulfate-polyacrylamide gels and transferred to polyvinylidene fluoride membranes with a pore size of 0.22 μm. Membranes were blocked with 5 % skim milk and incubated overnight at 4 °C with antibodies against LC3B (Cat.# ab192890; Abcam, Cambridge, UK), P62 (Cat.# HA721171, Huabio, Zhejiang, China), TFEB (Cat.# 13372-1-AP, Proteintech, Wuhan, China), LAMP1 (Cat.# 67300-1-IG, Proteintech, Wuhan, China), and β-actin (Cat.# 66009-1-IG, Proteintech, Wuhan, China). Horseradish peroxidase (HRP)-conjugated secondary antibodies were applied to the membranes (goat anti-rabbit IgG-HRP, Cat.# BA1054, BOSTER, Wuhan, China; goat anti-mouse IgG-HRP, Cat.# BA1050, BOSTER, Wuhan, China) for 1 h at room temperature and detected using an enhanced chemiluminescence substrate (Bio-Rad, Hercules, CA, USA). Images were analyzed using Image Lab software (Bio-Rad).

2.9. Quantitative reverse transcription-polymerase chain reaction (qRT-PCR)

Total RNA was extracted from intestinal tissues and cultured cells using a total RNA extraction kit (Cat.# 400-100-100T; GOONIE) and reverse transcribed into cDNA using random hexamers provided with the kit (Cat.# AE311-03; TransGen Biotech, Beijing, China). cDNA was analyzed using the Fast SYBR Green PCR Master Mix (Cat.# AQ601-02-V2, TransGen Biotech, Beijing, China) in an Applied Biosystems Quant Studio 5 instrument for the target genes (*MAPLC3B, SQSTM1, TFEB,* and *CTSD*; Tables S1–2). The relative expression of the target genes was normalized to that of β-actin or GAPDH and calculated as $2^{(Ct(\beta\text{-actin-gene of interest}))}$.

2.10. Immunofluorescence and immunohistochemistry staining

For immunofluorescence, cells or tissues were fixed and blocked before being incubated with primary antibodies against LC3B, P62, TFEB, and LAMP1 at 4 °C overnight. This was followed by a 2-h incubation with secondary antibodies, either Alexa Fluor 488-conjugated anti-mouse IgG (Cat.# 4408S, Cell Signaling Technology, Danvers, MA, USA) or Cy3-conjugated anti-rabbit IgG (Cat.# BA1032, BOSTER, Wuhan, China). The cells and sections were then counterstained with DAPI (Cat.#C0065, Solarbio, Wuhan, China). Images were acquired using a confocal laser scanning microscope (LSM900; Zeiss, Oberkochen, Germany) and analyzed with Zen 2.3 (blue edition) software (Zeiss, Oberkochen, Germany). Lysosomal volume was measured by incubating cells with 50 nM LysoTracker Red DND-99 (Cat.# 40739ES50; Yeasen, Shanghai, China) at 37 °C for 2 h to stain lysosomes.

For immunohistochemical staining, small intestinal sections were incubated with primary antibodies at 4 °C overnight, followed by incubation with secondary antibodies at 37 °C for 30 min. Cell nuclei were counterstained with hematoxylin. Images were captured using an Olympus optical microscope, and image analysis and quantification were conducted using Image J software (National Institutes of Health, Bethesda, MD, USA).

2.11. Statistical analysis

Data are presented as the mean ± standard error of the mean (SEM). A Student's t-test was used to compare two groups, while one-way analysis of variance (ANOVA) followed by Tukey's post-hoc test was applied for comparisons among three or more groups. The threshold for statistical significance was set at $p < 0.05$. Both in vitro and *in vivo* experiments were performed independently at least three times. Statistical differences were assessed using GraphPad Prism 8 software (GraphPad, San Diego, CA, USA).

3. Results

3.1. The ALP is impaired in infants with NEC

This study enrolled three infants with NEC, whose detailed characteristics are outlined in Table 1. To investigate differential gene expression patterns associated with the ALP, RNA-seq analyses were conducted on ileal tissues from preterm infants with and without NEC (serving as controls). A total of 2076 differentially expressed genes were identified ($p < 0.05$), with 455 upregulated and 1621 downregulated (Fig. 1A). The heatmap in Fig. 1B illustrates the 27 genes that were either up- or downregulated and are related to the ALP, comparing the control and NEC groups. The expression levels of *MAPLC3B* and *SQSTM1* (encoding LC3 and P62 protein, respectively), genes involved in autophagosome formation, were significantly increased in the NEC group relative to the control group, aligning with previous findings [27]. Notably, the expression levels of *TFEB* and *CTSD* (encoding TFEB and CTSD protein, respectively), genes associated with lysosomal biogenesis, were reduced in the NEC group. Furthermore, RT-PCR revealed markedly higher expression levels of *MAP1LC3B* ($p < 0.05$, Fig. 1C) and *SQSTM1* ($p < 0.05$, Fig. 1C), and lower expression levels of *TFEB* ($p < 0.001$, Fig. 1C) and *CTSD* ($p < 0.001$, Fig. 1C) compared to the control group. Additionally, H&E staining and TEM revealed a complete absence of epithelial structures, transmural necrosis (Fig. 1D) and ultrastructural changes in NEC tissues (Fig. 1E). Consistent with previous studies [16], we observed two giant autophagy -lysosomes in the NEC group, fewer in number than those in the control group (Fig. 1E). These findings suggest that aberrant autophagy in NEC is correlated with diminished lysosomal activity.

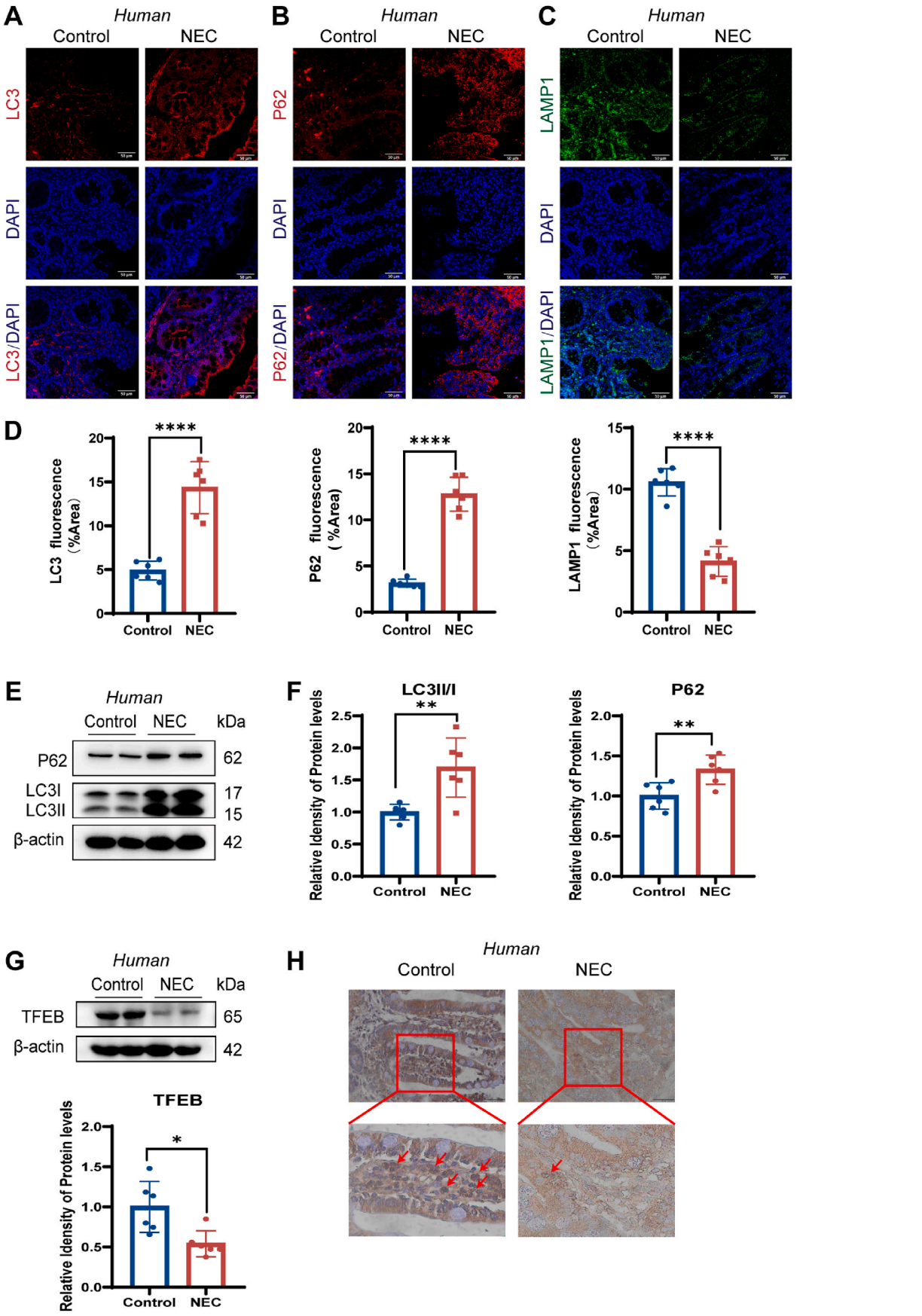

(caption on next page)

Fig. 2. Autophagy is active while lysosomal activity is compromised in NEC.
(A) Representative histological images of intestinal tissue, visualized by immunofluorescence staining for LC3B (red). Scale bar = 50 μm. **(B)** Immunofluorescence staining of ileal sections for P62 (red). Scale bar = 50 μm. **(C)** Immunofluorescence staining of ileal sections for LAMP1 (green). Scale bar = 50 μm. **(D)** Statistical analysis of the fluorescent area percentage for LC3B, P62, and LAMP1. Data are presented as the mean ± SD. ****$p < 0.0001$. **(E)** Expression levels of autophagy-related proteins (P62 and LC3II/LC3I) in NEC intestinal tissues, analyzed by Western blot and normalized to β-actin. **(F)** Densitometric analysis of Western blot bands for P62 and LC3II/LC3I, normalized to β-actin. Data are shown as the mean ± SD. **$p < 0.01$. **(G)** Expression of lysosome-related protein TFEB in NEC intestinal tissues, analyzed by Western blot and normalized to β-actin. Densitometric analysis of Western blot bands for TFEB, normalized to β-actin. Data are presented as the mean ± SD. *$p < 0.05$. **(H)** Representative immunohistochemistry (IHC) images displaying TFEB expression in ileal sections from NEC infants. Red arrows indicate TFEB expression in the nucleus.

3.2. Autophagy is active while lysosomal activity is compromised in infants with NEC

Autophagic flux, a term that precisely encapsulates the entire autophagy process, encompasses not only the enhancement of LC3 synthesis and lipidation but also the upregulation of autophagosome formation. Paramount to this concept is the flux through the entire system, including lysosomes and vesicles, culminating in the release of degradation products. This comprehensive process of autophagic flux is the gold standard for assessing autophagic activity [9]. Consequently, we conducted a protein-level investigation into the alterations of the ALP in NEC. Immunofluorescence staining revealed a significant increase in LC3 and P62 expression in intestinal tissues from NEC infants (Fig. 2A and B). Autophagic activity is contingent upon lysosomal function. Intriguingly, a reduction in lysosome quantity was noted, evidenced by a decrease in LAMP1 puncta in NEC (Fig. 2C). These results support the contention that, notwithstanding the initiation of autophagy in NEC, autophagic activity is impeded at NEC pathogenesis owing to deficits in lysosomal functionality and a reduction in lysosomal count.

We also quantified the expression levels of autophagy-lysosome-related proteins, including LC3II/LC3I and P62, in the intestinal tissues of NEC patients using Western blot analysis. A significant increase in the expression levels of LC3II/LC3I and P62 was observed in the NEC group (Fig. 2E and F), but significantly decreased expression levels of TFEB in the NEC group (Fig. 2G). Additionally, the expression and localization of TFEB in intestinal sections from NEC patients were also assessed using immunohistochemistry, which revealed markedly lower nuclear TFEB levels in the NEC group compared to the control group (Fig. 2H). Together, these data further suggested that the association of ALP abnormalities with NEC, which characterized by impaired autophagosome fusion and lysosomal dysfunction.

3.3. ITA preserves intestinal epithelial barriers to ameliorate NEC in mice

Given the regulatory role of ITA in the ALP [28] and the observed decrease in ITA levels in the serum of infants with NEC [21], we evaluated whether treatment with ITA could ameliorate NEC. Notably, in experiments with NEC mice administered ITA, there was a notable trend towards reduced NEC mortality with ITA administration (Fig. 3A and S1), particularly pronounced at a dosage of 40 mg/kg with ITA prophylactic treatment. Consistently, ITA also improved weight gain, disease severity, and decreased the expression levels of inflammatory factors, including IL-6 and IL-1β, and tended to mitigate oxidative stress levels in the NEC model (Fig. 3B–E and S2A-B). Furthermore, ITA increased the expression levels of ZO-1 and occludin-1 (Fig. 3F and G), which are biomarkers of tight junctions. Collectively, these findings suggest that ITA significantly alleviates the pathological features of NEC and preserves the integrity of the intestinal epithelial barrier.

3.4. ITA administration enhances autophagy-lysosomal function in mice with NEC

Subsequently, we examined whether the protective effect of ITA against NEC was associated with the ALP. We observed enhanced fusion of autophagosomes and lysosomes in ITA-treated mice with NEC (Fig. 4A). Concurrently, the ITA-treated group exhibited reduced expression levels of LC3II/LC3I ($p < 0.05$) and P62 ($p < 0.001$) compared to the NEC group (Fig. 4B and C). Furthermore, the expression levels of TFEB were significantly higher in the NEC + ITA group than in the NEC group ($p < 0.01$; Fig. 4D). We also quantified the expression levels of LC3 and LAMP1 using immunofluorescence staining, revealing an increased degree of LC3 and LAMP1 colocalization in the ITA-treated group compared to the NEC group (Fig. 4E). Moreover, ITA treatment also led to improved lysosomal degradation function, as indicated by the reduced expression level of P62 in the NEC + ITA group (Fig. 4F).

3.5. ITA administration improves autophagic activity and autophagy-lysosomal function in HIEC6 cells under inflammatory conditions

To investigate how ITA affects ALP in NEC, we utilized HIEC6 cells to explore the activation levels of autophagy under inflammatory conditions. Immunoblotting analysis demonstrated that autophagy activation commenced during the early phase of inflammatory stimulation in HIEC6 cells, as evidenced by a notable increase in the expression levels of LC3II/LC3I and P62 from 0 to 48 h. Conversely, the expression level of TFEB in I-HIEC6 cells decreased from 0 to 48 h, with significant differences observed from 12 to 48 h (Fig. 5A and B). Intriguingly, the viability of HIEC6 cells was ITA concentration-dependent (Fig. 5C). We subsequently assessed the anti-inflammatory effects of ITA treatment, finding a significant reduction in the levels of inflammatory factors (IL-6 and IL-1β) measured using qRT-PCR at an ITA dose of 100 μM (Fig. 5D).

Next, we examined autophagosome-lysosome fusion and lysosomal function in ITA-treated I-HIEC6 cells. As shown in Fig. 5E, ITA treatment significantly decreased expression level of LC3 and increased expression level of LAMP1 at 48 h. Additionally, we assessed lysosomal function using LysoTracker staining of lysosomes. As depicted in Fig. 5F, ITA treatment decreased lysosomal volume and increased the number of lysosomes, similar to our findings of enlarged lysosomes in the ultrastructure of mouse and human intestinal epithelial cells from individuals with NEC. These data indicate that ITA ameliorates NEC by modulating the ALP.

3.6. ITA treatment increases autophagic flux under inflammatory conditions

To further elucidate the impact of ITA on autophagic flux in the context of NEC, we employed chloroquine (CQ), which can partially inhibit the fusion of autophagosomes with lysosomes [9]. Our findings demonstrated that ITA treatment significantly increased the accumulation of LC3II and p62 in the ITA-treated NEC group following CQ adminstration (Fig. 6A and B). Consistently, the expression levels of LC3II/LC3I and P62 were elevated in ITA-treated I-HIEC6 cells subsequent to CQ treatment (Fig. 6C and D). In comparison to ITA-treated mice with NEC, those co-treated with CQ exhibited increased LC3 expression levels, yet there was no enhancement in the degree of colocalization of LC3 and LAMP1 (Fig. 6E). A similar pattern was observed in HIEC6 cells under inflammatory conditions following cotreatment with ITA and CQ (Fig. 6F). Collectively, these results suggest that ITA stimulates autophagic flux in both mice with NEC and HIEC6 cells under inflammatory conditions.

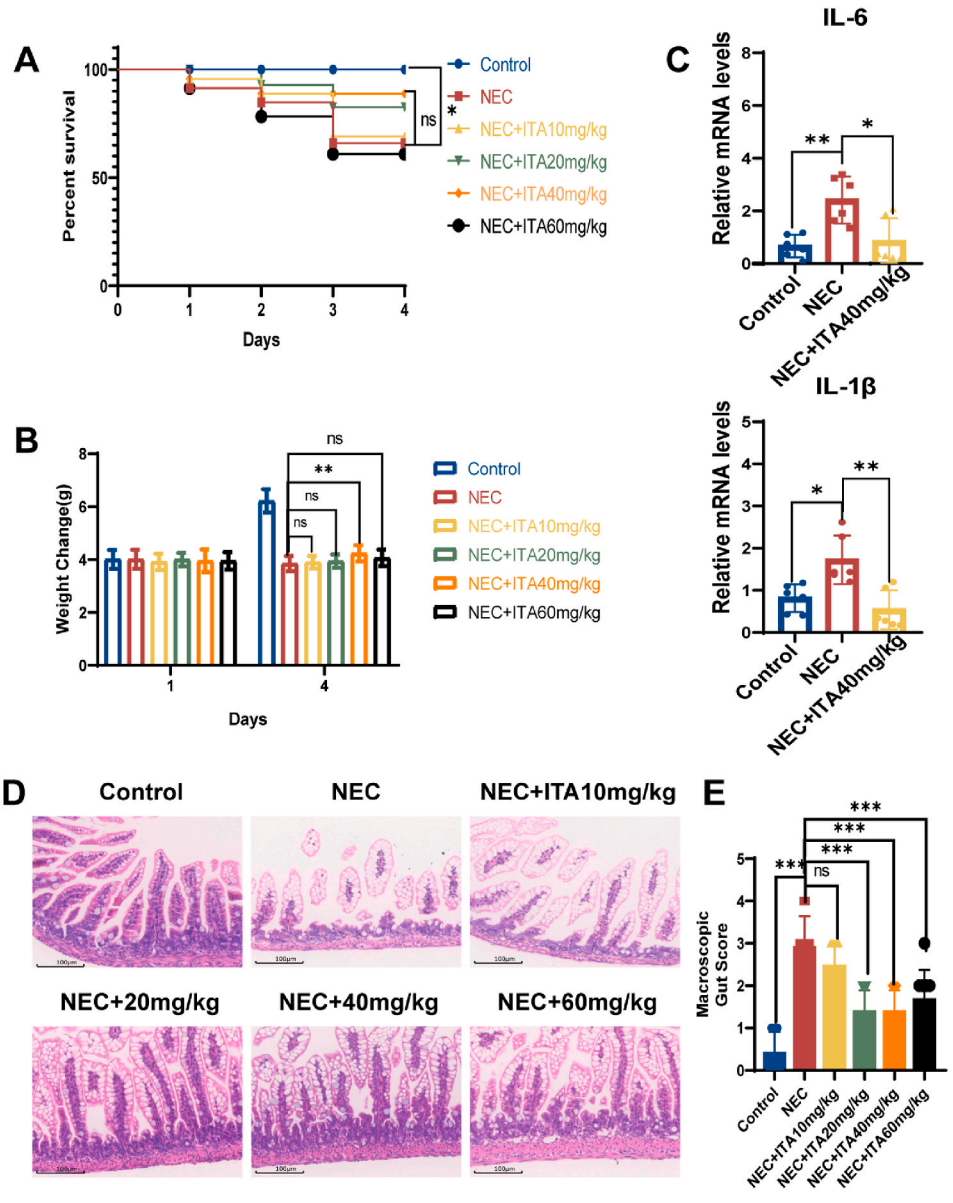

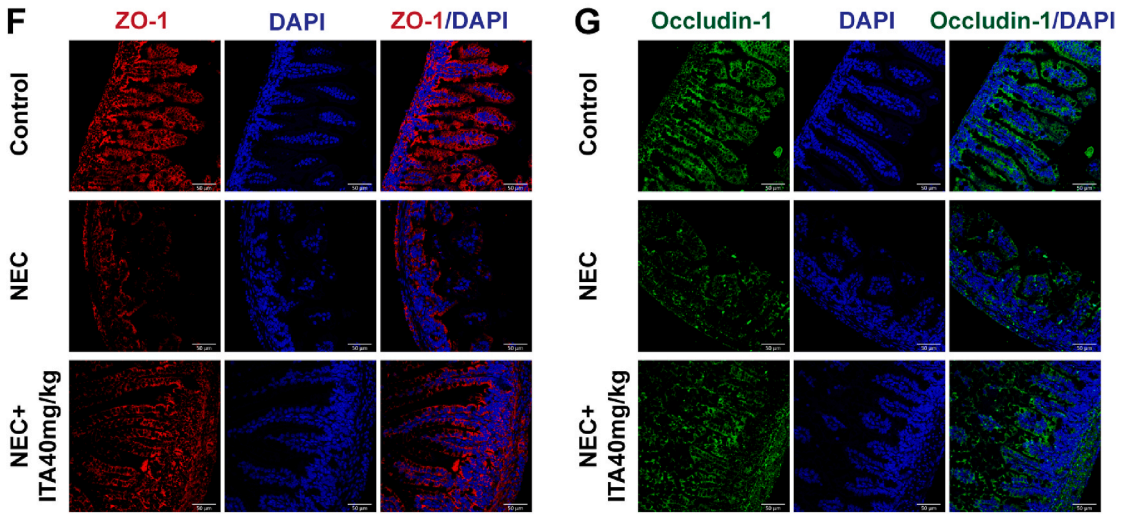

(caption on next page)

Fig. 3. Prophylactic therapeutic effects of ITA in mouse pups with NEC.
(A) Kaplan-Meier survival curves and log-rank tests were utilized to assess survival rates among control, NEC, and NEC pups treated with varying concentrations of ITA. N = 15 animals/group, with ns: $p > 0.05$; *$p < 0.05$. **(B)** Weight changes in mouse pups across control, NEC, and NEC + ITA groups. **$p < 0.01$. **(C)** Expression levels of inflammatory factors IL-6 and IL-1β in control, NEC, and NEC + ITA (40 mg/kg) groups, measured by qRT-PCR and normalized to β-actin. Data are presented as the mean ± SD. *$p < 0.05$, **$p < 0.01$. **(D)** Representative histology (H&E staining) of ileal sections from control, NEC, and NEC + ITA groups in mouse pups. Scale bar = 100 μm. **(E)** Macroscopic gut score for the ilea in control, NEC, and NEC + ITA groups, presented as the mean ± SD. ns: $p > 0.05$; ***$p < 0.001$. **(F)** Fluorescence staining of ileal sections showing ZO-1 (red), DAPI (blue) after ITA prophylactic treatment (40 mg/kg). Scale bar = 50 μm. **(G)** Fluorescence staining of ileal sections showing Occludin-1 (green), DAPI (blue) after ITA prophylactic treatment (40 mg/kg). Scale bar = 50 μm.

3.7. ITA increases the nuclear translocation of TFEB to enhance the ALP under inflammation conditions

Given that the inactivation of mTORC1 under energy stress conditions induces dephosphorylation and nuclear translocation of TFEB, along with increased expression levels of LC3 and P62 [29], and considering that ITA can promote the ALP by increasing TFEB expression levels and TFEB nuclear translocation [30], we investigated whether ITA enhances autophagic flux by modulating TFEB in NEC. Notably, in mice with NEC, treatment with ITA resulted in a significant increase in the nuclear localization of TFEB (Fig. 7A and B). A similar pattern was observed in HIEC6 cells incubated under inflammatory conditions with or without ITA treatment(Fig. 7C and D). Furthermore, the expression and localization of TFEB in the intestine of NEC mice were analyzed using immunohistochemistry, showing a marked elevation in nuclear TFEB localization after ITA treatment (Fig. 7E). We also examined the expression of TFEB in HIEC6 cells incubated under inflammatory conditions with or without ITA treatment, observing a significant increase in the fluorescence intensity of nuclear TFEB in HIEC6 cells under inflammatory conditions following ITA treatment (Fig. 7F). Taken together, these results indicate that TFEB, increased by ITA, contributes to the ALP and ultimately ameliorates NEC.

4. Discussion

NEC is among the most prevalent and lethal conditions affecting neonates. The pathophysiology of NEC is marked by the disruption of intestinal architecture and necrosis of enterocytes due to excessive inflammation, leading to intestinal barrier dysfunction [1]. Prior research has highlighted that excessive inflammation, stemming from a reduction in regulatory T cells (Treg) and an increase in Th17 cells, is a pivotal factor in NEC [22]. Over recent years, a growing body of evidence has underscore a close link between autophagy and NEC. Notably, the progression of NEC is contingent upon TLR4-dependent autophagy enhancement within the intestinal epithelium [31,32]. Substantial evidence indicates that autophagy is crucial for maintaining celluar homoeostasis and differentiation, especially under stressful conditions. This cellular process is vital for eliminating invading pathogens and modulating the inflammatory response triggered by various pathogens or their components. Impaired autophagy can result in uncontrolled infections and heightened inflammation [33]. Recent studies have established that the excessive inflammation and apoptosis of intestinal epithelial cells in NEC are intimately associated with hyperactivated autophagy. However, the specific role of autophagy in the heightened inflammation associated with NEC remains elusive. Consequently, the primary objectives of this study were to delineate the potential molecular mechanisms of autophagy in intestinal epithelial cells under inflammatory conditions in NEC and to establish the connection between autophagy and the intestinal barrier in NEC, potentially offering a new therapeutic target for reversal of NEC.

Autophagy is the principal intracellular degradation mechanism tasked with transportation and degradation of cytoplasmic components within the lysosome. It is categorized into three main types: macroautophagy, microautophagy, and chaperone-mediated autophagy. Among these, marcroautophagy is considered the predominant form of autophagy. This highly inducible process is triggered by conditions such as starvation and various forms of stress, leading to a rapid increase in autophagosome formation. The autophagosome then fuses with the lysosome to form an autolysosome, which is responsible for degrading its contents. However, the primary role of autophagy extends beyond the mere elimination of cellular constituents; it functions as a dynamic recycling system that generates new building blocks and provides energy crucial for cell renewal and the maintenance of homeastasis [34]. During autophagy, LC3 II is targeted to the membranes of autophagosomes and/or autolysosomes, making it a valuable marker for assessing autophagy levels within cells [35]. Consistent with previous studies, we found that the expression level of LC3 II was increased at both the protein and gene levels in NEC compared to controls, potentially due to autophagosome accumulation in NEC, including inhibition of autophagosome-lysosome fusion and/or lysosome-mediated degradation. To investigate the mechainsm responsible for the increased LC3 II levels in patients with NEC, we performed RNA-seq analysis and enriched ALP-related genes using ileal tissue from neonates with and without NEC (controls). The results revealed elevated expression levels of the autophagy-related genes *MAPLC3B* and *SQSTM1*, and decreased expression levels of the lysosomal genes *CTSD* and *TFEB*. TEM identified two enlarged autophagic lysosomes in NEC intestinal epithelial cells, a reduced number compared to control cells. When assessing lysosomal function, we noted an increase in P62 expression (indicating inhibited lysosomal degradation) and a decrease in LAMP1 expression (indicating a reduced number of lysosomes). These findings underscore the crucial role of the autophagy-lysosome systemin the pathogenesis of NEC.

Lysosome-mediated autophagy is indeed a primary intracellular degration process. Autophagosome-lysosome fusion and lysosomal function are recognized as the most critical factors in autophagic degradation [8,34]. Additionally, TFEB has been identified as a key regulator of lysosome biogenesis and autophagy by modulating the expression of genes associated with these processes, thereby supervising the entire autophagic cascade [36]. In our current study, the expression level of TFEB was decreased in patients with NEC. Consequently, we investigated the significance of the ALP in the pathogenesis of NEC using both an in vitro cellular inflammatory model and *in vivo* NEC animal models. We assessed autophagy-lysosome-related protein and gene expression levels in the mouse modelof NEC, and the results were consistent with those observed in patients with NEC, showing increased expression levels of LC3II and p62, and decreased expression levels of LAMP1. These findings align with those of previous studies [37,38]. In this study, HIEC6 cells were incubated with TNF-α (10 ng/mL) and IL-1β (5 ng/mL) to creat an inflammatory environment, which poses a significant risk in the pathological process of NEC. As cellular autophagy levels fluctuate under inflammatory conditions during incubation [26], we quantified autophagy levels in HIEC6 cells at 0, 6, 12, 24 and 48 h under inflammatory conditions. Cells incubated for 48 h under inflammatory conditions were designated as I-HIEC6 cells, while those incubated under normal conditions for 48 h served as control HIEC6 cells. We observed that the expression levels of LC3B and p62 in the I-HIEC6 group increased over time, while the expression level of TFEB gradually decreased. In summary, our study revealed that excessive autophagy activation and lysosomal dysfunction, associated with inhibition of the ALP due to reduced TFEB expression levels, are characteristic of the hyperinflammatory response in NEC.

Autophagy is a complex and dynamic multi-step process that includes several key stage, such as nucleation and initiation, elongation, maturation, and the degradation and recycling of cellular components

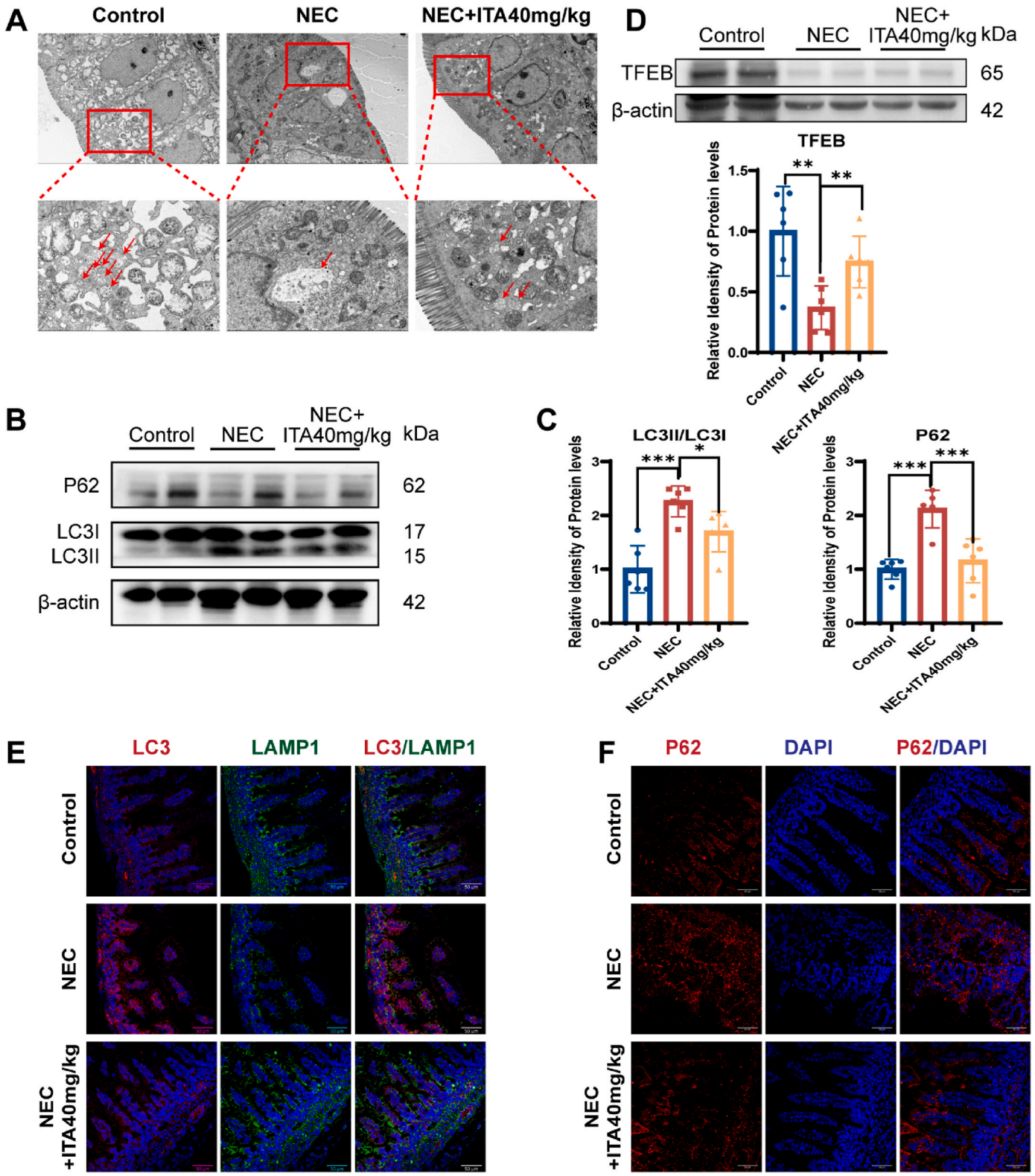

Fig. 4. ITA treatment enhances autophagosome-lysosome fusion and lysosomal functions in mouse pups with NEC.
(A) Morphological characteristics of autophagy ultrastructure in control, NEC, and NEC + ITA (40 mg/kg) groups, as observed by TEM (top panel, scale bar = 5 μm; bottom panel, scale bar = 2 μm; red arrows indicate autolysosomes). **(B)** ITA modulates the expression of autophagy-related proteins (P62 and LC3II/LC3I) in NEC mice. N = 6 animals/group. (Western blot, normalized to β-actin). **(C)** Protein levels of P62 and LC3II/LC3I were quantified by Western blot and normalized to β-actin. Data are presented as the mean ± SD. *$p < 0.05$, ***$p < 0.001$. **(D)** Expression of lysosome-related protein TFEB in NEC mice, analyzed by Western blot. N = 6 animals/group. Densitometric analysis of Western blot bands for TFEB, normalized to β-actin, is depicted. Data are presented as the mean ± SD. **$p < 0.01$. **(E)** ITA promotes autophagosome-lysosome fusion in NEC mice, evidenced by immunofluorescence analysis of LC3 (red) and LAMP1 (green). Scale bar = 50 μm. **(F)** ITA ameliorates lysosomal functions in NEC mice, as measured by immunofluorescence analysis of P62 (red). Scale bar = 50 μm.

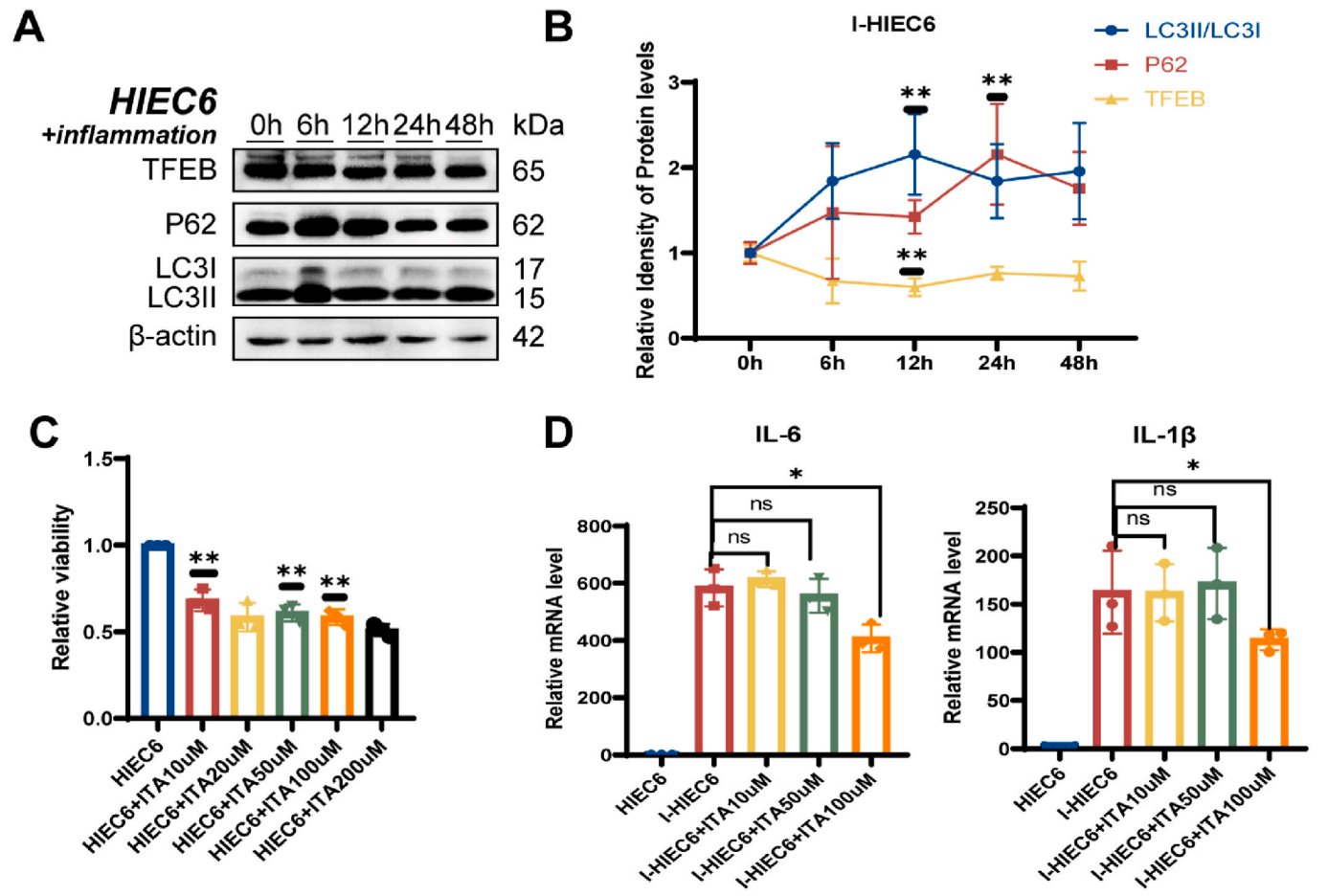

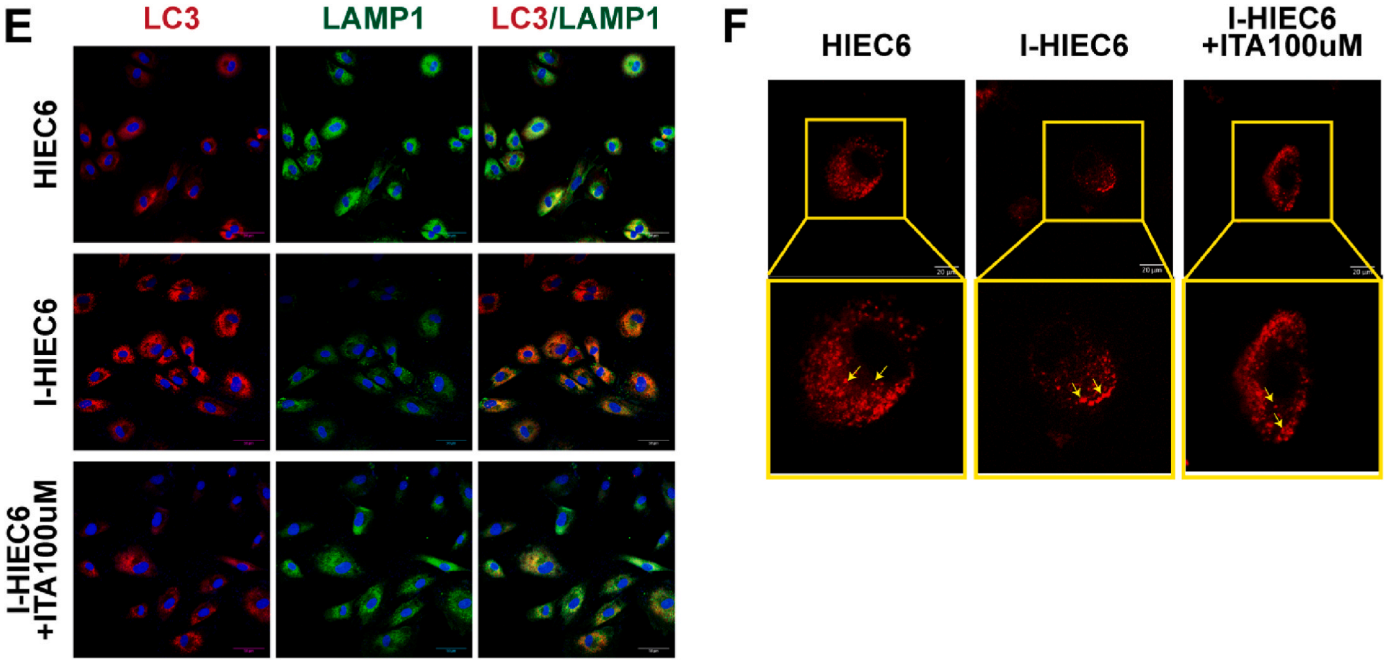

(caption on next page)

Fig. 5. Incubation of HIEC6 under inflammatory conditions leads to abnormal autophagy levels, but ITA improves autophagic activity and autophagy-lysosomal function.
(**A**) Expression levels of autophagy-related proteins (LC3, P62 and TFEB) in HIEC6 cells under inflammatory conditions, assessed by Western blot analysis at 0, 6, 12, 24 and 48 h, and normalized to β-actin. (**B**) Western blot data from **(A)** are expressed as fold changes relative to protein levels at 0 h. Data are shown as the mean ± S. D. (n = 3), ***p < 0.001 and ****p < 0.0001. (**C**) Viability of HIEC6 cells treated with varying concentrations of ITA, evaluated using the CCK-8 kit according to the manufacturer's protocol. (**D**) Expression of inflammatory factor genes (IL-6 and IL-1β) in HIEC6 cells, I-HIEC6 cells and ITA-treated groups at varying concentrations, measured by qRT-PCR and normalized to GAPDH. Data are shown as the mean ± SD. *$p < 0.05$. (**E**) ITA treatment promoted autophagosome-lysosome fusion in HIEC6 cells under inflammatory conditions at 48h, as shown by an immunofluorescence analysis of LC3(red) and LAMP1(green). Scale bar = 50 μm. (**F**) ITA treatment improved lysosomal functions in HIEC6 cells under inflammatory conditions at 48h, indicated by amelioration of lysosome volume decrease, as determined by LysoTracker staining (red: LysoTracker-stained lysosomes; yellow arrows, lysosomes; top panel, scale bar = 20 μm).

[39]. Therefore, there is an urgent need for effective strategies that target specific phases of autophagy rather than the entire process. This study underscores the importance of modulating the autophagy-lysosome system as a potential therapeutic approach. However, it is important to note that the efficacy of therapies focused on lysosomal components has been validated in only a limited number of clinical trials [40]. Therefore, it is crucial to explore new and effective strategies that target the autophagy-lysosome system to counteract the excessive inflammation-induced abnormalities in autophagy associated with NEC.

Recent studies have demonstrated that differential metabolite levels are associated with changes in specific clinical indicators. For example, in Parkinson's disease, certain metabolites can activate mitophagy and autophagy, protecting cells from degeneration [41]. In addition, a reduction in ITA levels may serve as a diagnostic indicator for NEC [21,30]. ITA, a metabolite of TCA cycle, is produced by the decarboxylation of cis-aconitic acid catalyzed by the enzyme ACOD1 in the mitochondrial matrix. When the TCA cycle is disrupted, macrophages accumulate ITA, which exhibits immunomodulating effects in the body. In our study, prophylactic administration of ITA was more effective in improving NEC mortality rates than therapeutic administration of ITA. Additionally, ITA significantly alleviated inflammation, intestinal tissue disorganization, and intestinal barrier damage in mice with NEC. Over the past few years, scientific studies have shown that ITA plays a crucial role in the interplay between metabolism, inflammation, oxidative stress and immune responses [11]. Michopoulos et al. found that ITA was strongly associated with disease progression and could be used as a disease marker for rheumatoid athritis [42]. During respiratory syncytial virus (RSV) infection, ITA is responsible for the production of reactive oxygen species (ROS) and inflammatory cytokines, leading to lung tissue damage; IRG1−/− mice show effective inhibition of RSV infection [43]. ITA also elevates glutathione levels in the brain, reduces the levels of ROS and reactive nitrogen species, and improves hemodynamics, while reducing leukocyte adhesion, thus improving neurological function [44]. In the acidic phagolysosome, itaconic acid functions as a potent antimicrobial agent against multidrug-resistant *Staphylococcus aureus* strains, acting as a weak acid that induces acidic, oxidative, and electrophilic stress responses [45]. In our study, we also observed a trend towards reduced oxidative stress levels following ITA treatment in NEC mice. And Loi et al. have also demonstrated that the impact of ITA on intracellular pH is dose-dependent. Moreover, Berezhnov et al. demonstrated that intracellular pH exerts a regulatory influence on autophagy and mitochondrial autophagy [46]. In our in vitro experiments, we utilized a concentration of 100 μM itaconic acid and concluded that this dosage was unlikely to alter intracellular pH. It's worth noting that we demonstrated the protective effect of ITA treatment on the intestinal barrier in NEC, and determined the mechanism by which ITA improves the ALP by modulating TFEB.

The ALP is crucial for maintaining cellular homeostasis and providing organ protection. Our study aimed to elucidate the impact of ITA on the ALP by assessing autophagy and autophagic flux in ITA-treated mice with NEC and in I-HIEC6 cells. We observed that ITA treatment significantly reduced the expression levels of LC3 and P62, indicating a decrease in autophagosome accumulation, and promoted autophagic flux in both NEC mice and I-HIEC6 cells. Furthermore, ITA treatment improved autophagosome-lysosome fusion in NEC mice, as evidenced by an increased number and improved ultrastructural morphology of autophagic lysosomes determined by TEM. Additionally, ITA enhanced lysosomal degradation and mitigated the increase in lysosome volume in both NEC mice and I-HIEC6 cells. TFEB, primarily regulated by the ALP, is known to facilitate lysosomal biogenesis and bacterial clearance during the innate immune response, thereby improving the ALP [47]. Our data revealed an enhanced nuclear localization of TFEB along with elevated expression levels of autophagy-related and lysosome-related proteins influenced by TFEB in ITA-treated mice and I-HIEC6 cells. Collectively, these results suggest that ITA induced changes in the ALP, including increased fusion of autophagosomes and lysosomes, rejuvenation of lysosomal functionality, and clearance of autophagic substrates.

However, the present study is subjected to several limitations. We did not directly knock down the sites interacting with ITA or inhibit the nuclear translocation of TFEB to verify the role of ITA in the ALP in mice with NEC or HIEC6 cells under inflammatory conditions. Therefore, it is still unclear whether TFEB influences the ALP in the context of NEC. In future studies, we will further investigate the molecular mechanisms for the interaction between ITA and TFEB in response to excessive inflammation in NEC by knocking down or overexpressing TFEB. The therapeutic concentrations of ITA and the safety of the drug, especially its metabolism in the neonatal period, need to be further investigated to ensure a safe situation for neonatal use. Under these circumstances, it is essential to conduct a thorough investigation of the interactions between ITA and cells, as well as to explore the pharmacological effects of ITA for potential future therapeutic applications.

In conclusion, we found that ITA upregulated the expression of TFEB and enhanced the ALP, thereby preserving the integrity of the intestinal epithelial barrier in NEC. These findings suggest that modulating the ALP, particularly through ITA, could offer a promising therapeutic approach to mitigate the pathogenesis of NEC.

CRediT authorship contribution statement

Baozhu Chen: Writing – original draft, Methodology, Investigation, Conceptualization. **Yufeng Liu:** Writing – original draft, Methodology, Investigation. **Shunchang Luo:** Writing – original draft, Methodology, Investigation. **Jialiang Zhou:** Resources, Project administration, Formal analysis, Data curation. **Yijia Wang:** Methodology, Investigation, Formal analysis. **Qiuming He:** Resources, Methodology, Investigation. **Guiying Zhuang:** Resources, Funding acquisition, Formal analysis. **Hu Hao:** Writing – review & editing, Supervision, Conceptualization. **Fei Ma:** Writing – review & editing, Funding acquisition, Conceptualization. **Xin Xiao:** Writing – review & editing, Supervision, Conceptualization. **Sitao Li:** Writing – review & editing, Supervision, Funding acquisition, Data curation, Conceptualization.

Funding

This work was supported by the National Natural Science Foundation of China (Grants 82271736to Sitao Li, 82371713to Fei Ma, and 82071680to Hu Hao), Guangdong Basic and Applied Basic Research Foundation (Grants 2024A1515010520to Sitao Li,

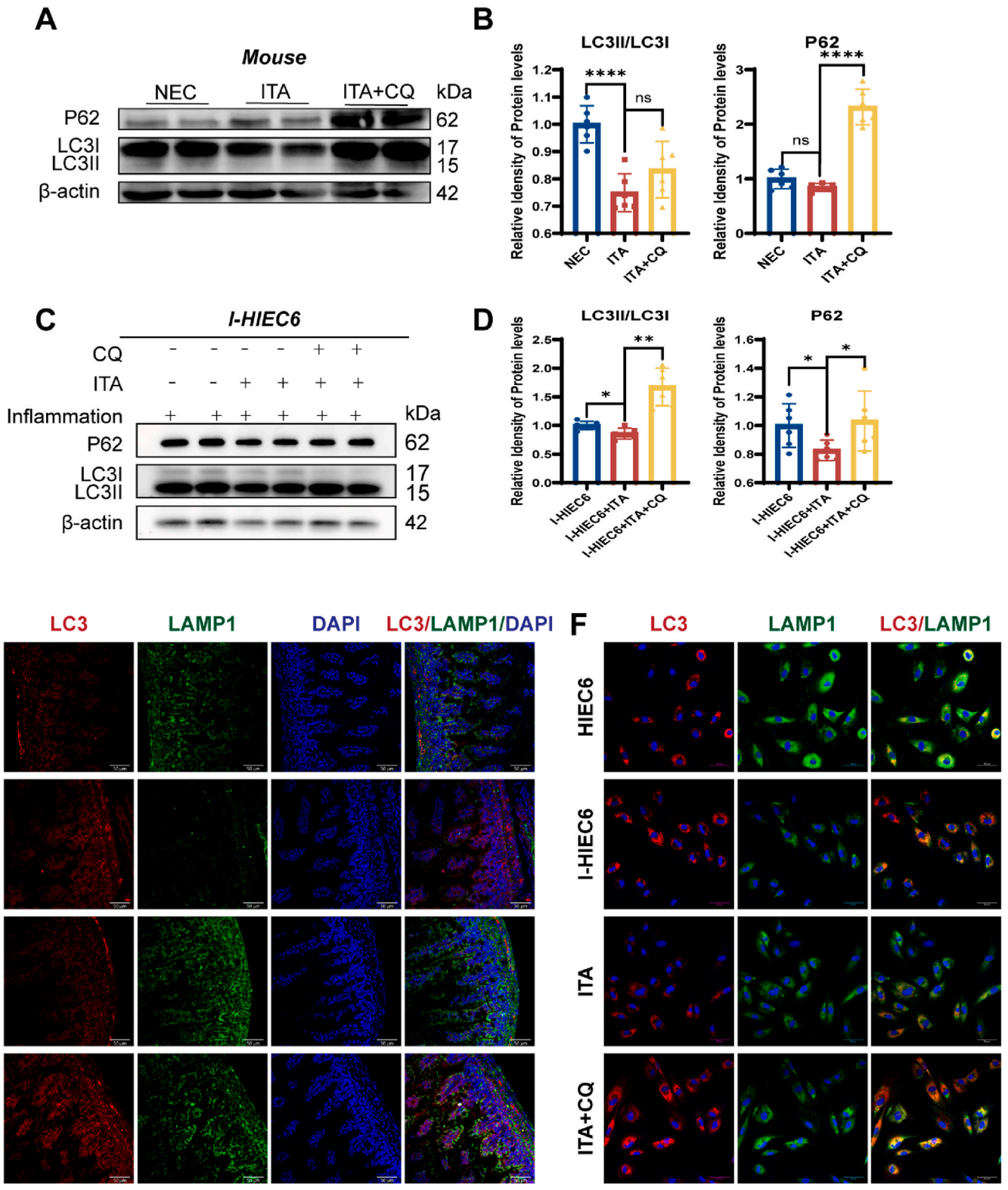

Fig. 6. ITA treatment promotes autophagy flux in NEC mice and I-HIEC6 cells under inflammatory conditions.
(A) Western blotting analysis of P62 and LC3II/LC3I in NEC mice with ITA(40 mg/kg) and chloroquine(30 mg/kg). N = 6 animals/group. **(B)** Densitometric analysis of Western blot bands from **(A)**, normalized to β-actin. Data are shown as the mean ± SD. ***$p < 0.0001$. **(C)** Cells were pretreated with chloroquine (CQ, 15uM) for 48 h to inhibit autophagosome-lysosome fusion prior to collection for Western blot analysis. (n = 3) **(D)** Densitometric analysis of Western blot bands from **(C)**, normalized to β-actin. Data are presented as the mean ± SD. *$p < 0.05$ and **$p < 0.01$. **(E)** Representative histological images from immunofluorescence staining of ileal sections showing LC3(red), LAMP1(green) and DAPI (blue). Scale bar = 50 μm. **(F)** Immunofluorescence staining of HIEC6 cells showing LC3(red), LAMP1 (green) and DAPI (blue). Scale bar = 50 μm.

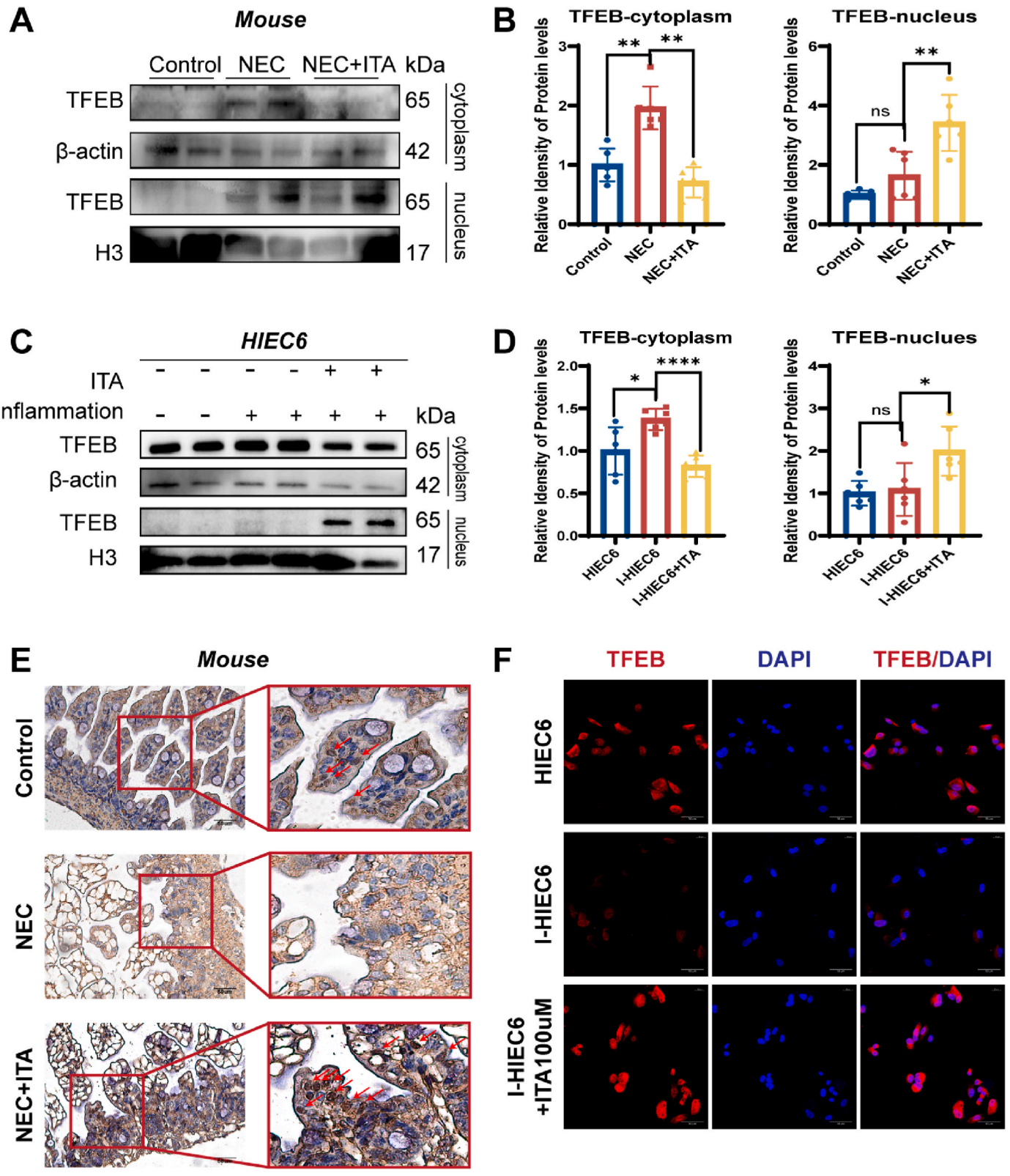

Fig. 7. ITA promotes nuclear translocation of TFEB under inflammatory conditions.
(A) Western blot analysis of TFEB levels in the cytoplasm and nucleus of NEC mice and ITA-treated groups. Densitometric analysis of Western blot bands is normalized to β-actin and H3. N = 6 animals/group. **(B)** Densitometric analysis of Western blot bands from **(A)**, normalized to β-actin and H3. Data are presented as the mean ± SD. $^{**}p < 0.01$. **(C)** Western blotting analysis of TFEB levels in the cytoplasm and nucleus of HIEC6 cells under inflammatory conditions. (n = 3) **(D)** Densitometric analysis of Western blot bands from **(C)**, normalized to β-actin. Data are presented as the mean ± SD. **(E)** Representative IHC images showing TFEB expression in ileal sections from NEC and ITA-treated NEC groups. Red arrows indicate TFEB expression levels in the nucleus. **(F)** Immunofluorescence staining of HIEC6 cells under inflammatory conditions with ITA treatment, showing TFEB(red) and DAPI(blue). Scale bar = 50 μm.

2022A1515010388to Fei Ma, 2023A1515012569to Hu Hao), the Science and Technology Projects of Social Development in Zhuhai (Grants 2320004000001and 2220004000299to Fei Ma), Huadu District Basic and Applied Basic Research District Institute(Grant 23HDQYLH25 to Guiying Zhuang), and Medical Scientific Research Foundation of Guangdong Province of China (Grant B2023374 to Jialiang Zhou).

Declaration of competing interest

The authors declare that they have no known competing financial interests or personal relationships that could have appeared to influence the work reported in this paper.

Appendix A. Supplementary data

Supplementary data to this article can be found online at https://doi.org/10.1016/j.freeradbiomed.2024.11.035.

References

[1] J. Neu, W.A. Walker, Necrotizing enterocolitis, N. Engl. J. Med. 364 (2011) 255–264, https://doi.org/10.1056/NEJMra1005408.
[2] J. Neu, Necrotizing enterocolitis: the future, Neonatology 117 (2020) 240–244, https://doi.org/10.1159/000506866.
[3] C. Zozaya, I. García González, A. Avila-Alvarez, N. Oikonomopoulou, T. Sánchez Tamayo, E. Salguero, M. Saenz De Pipaón, F. García-Muñoz Rodrigo, M.L. Couce, Incidence, treatment, and outcome trends of necrotizing enterocolitis in preterm infants: a multicenter cohort study, Front. Pediatr. 8 (2020) 188, https://doi.org/10.3389/fped.2020.00188.
[4] J. Shulhan, B. Dicken, L. Hartling, B.M. Larsen, Current knowledge of necrotizing enterocolitis in preterm infants and the impact of different types of enteral nutrition products, Adv. Nutr. 8 (2017) 80–91, https://doi.org/10.3945/an.116.013193.
[5] J. Neu, Necrotizing enterocolitis: the mystery goes on, Neonatology 106 (2014) 289–295, https://doi.org/10.1159/000365130.
[6] C. Bazacliu, J. Neu, Necrotizing enterocolitis: long term complications, Curr. Pediatr. Rev. 15 (2019) 115–124, https://doi.org/10.2174/1573396315666190312093119.
[7] E.G. Foerster, T. Mukherjee, L. Cabral-Fernandes, J.D.B. Rocha, S.E. Girardin, D. J. Philpott, How autophagy controls the intestinal epithelial barrier, Autophagy 18 (2022) 86–103, https://doi.org/10.1080/15548627.2021.1909406.
[8] H. Martini-Stoica, Y. Xu, A. Ballabio, H. Zheng, The autophagy-lysosomal pathway in neurodegeneration: a TFEB perspective, Trends Neurosci. 39 (2016) 221–234, https://doi.org/10.1016/j.tins.2016.02.002.
[9] D.J. Klionsky, A.K. Abdel-Aziz, S. Abdelfatah, M. Abdellatif, A. Abdoli, S. Abel, H. Abeliovich, Guidelines for the use and interpretation of assays for monitoring autophagy (4th edition) [1], Autophagy 17 (2021) 1–382, https://doi.org/10.1080/15548627.2020.1797280.
[10] Y. Wang, W.-D. Le, Autophagy and ubiquitin-proteasome system, in: Z.-H. Qin (Ed.), Autophagy Biol. Dis., Springer Singapore, Singapore, 2019, pp. 527–550, https://doi.org/10.1007/978-981-15-0602-4_25.
[11] F. Gros, S. Muller, The role of lysosomes in metabolic and autoimmune diseases, Nat. Rev. Nephrol. 19 (2023) 366–383, https://doi.org/10.1038/s41581-023-00692-2.
[12] M. Sardiello, M. Palmieri, A. di Ronza, D.L. Medina, M. Valenza, V.A. Gennarino, C. Di Malta, F. Donaudy, V. Embrione, R.S. Polishchuk, S. Banfi, G. Parenti, E. Cattaneo, A. Ballabio, A gene network regulating lysosomal biogenesis and function, Science 325 (2009) 473–477, https://doi.org/10.1126/science.1174447.
[13] F. Wang, S. Muller, Manipulating autophagic processes in autoimmune diseases: a special focus on modulating chaperone-mediated autophagy, an emerging therapeutic target, Front. Immunol. 6 (2015) 252, https://doi.org/10.3389/fimmu.2015.00252.
[14] A.J. Monteith, S. Kang, E. Scott, K. Hillman, Z. Rajfur, K. Jacobson, M.J. Costello, B.J. Vilen, Defects in lysosomal maturation facilitate the activation of innate sensors in systemic lupus erythematosus, Proc. Natl. Acad. Sci. U.S.A. 113 (2016) E2142–E2151, https://doi.org/10.1073/pnas.1513943113.
[15] K.G. Lassen, C.I. McKenzie, M. Mari, T. Murano, J. Begun, L.A. Baxt, G. Goel, E. J. Villablanca, S.-Y. Kuo, H. Huang, L. Macia, A.K. Bhan, M. Batten, M.J. Daly, F. Reggiori, C.R. Mackay, R.J. Xavier, Genetic coding variant in GPR65 alters lysosomal pH and links lysosomal dysfunction with colitis risk, Immunity 44 (2016) 1392–1405, https://doi.org/10.1016/j.immuni.2016.05.007.
[16] M. Yamoto, M. Alganabi, S. Chusilp, D. Lee, Y. Yazaki, C. Lee, B. Li, A. Pierro, Lysosomal overloading and necrotizing enterocolitis, Pediatr. Surg. Int. 36 (2020) 1157–1165, https://doi.org/10.1007/s00383-020-04724-x.
[17] J.Y. Guo, H.-Y. Chen, R. Mathew, J. Fan, A.M. Strohecker, G. Karsli-Uzunbas, J. J. Kamphorst, G. Chen, J.M.S. Lemons, V. Karantza, H.A. Coller, R.S. Dipaola, C. Gelinas, J.D. Rabinowitz, E. White, Activated Ras requires autophagy to maintain oxidative metabolism and tumorigenesis, Genes Dev. 25 (2011) 460–470, https://doi.org/10.1101/gad.2016311.
[18] J. Domínguez-Andrés, B. Novakovic, Y. Li, B.P. Scicluna, M.S. Gresnigt, R.J. W. Arts, M. Oosting, S.J.C.F.M. Moorlag, L.A. Groh, J. Zwaag, R.M. Koch, R. Ter Horst, L.A.B. Joosten, C. Wijmenga, A. Michelucci, T. van der Poll, M. Kox, P. Pickkers, V. Kumar, H. Stunnenberg, M.G. Netea, The itaconate pathway is a central regulatory node linking innate immune tolerance and trained immunity, Cell Metabol. 29 (2019) 211–220.e5, https://doi.org/10.1016/j.cmet.2018.09.003.
[19] A. Michelucci, T. Cordes, J. Ghelfi, A. Pailot, N. Reiling, O. Goldmann, T. Binz, A. Wegner, A. Tallam, A. Rausell, M. Buttini, C.L. Linster, E. Medina, R. Balling, K. Hiller, Immune-responsive gene 1 protein links metabolism to immunity by catalyzing itaconic acid production, Proc. Natl. Acad. Sci. U.S.A. 110 (2013) 7820–7825, https://doi.org/10.1073/pnas.1218599110.
[20] X. Liu, X. Zheng, Y. Lu, Q. Chen, J. Zheng, H. Zhou, TFEB dependent autophagy-lysosomal pathway: an emerging pharmacological target in sepsis, Front. Pharmacol. 12 (2021) 794298, https://doi.org/10.3389/fphar.2021.794298.
[21] F. Wang, G. Wang, W. Li, C. Xu, Z. Zeng, Y. Zhou, Analysis of serum metabolism in premature infants before and after feeding using GC–MS and the relationship with necrotizing enterocolitis, Biomed. Chromatogr. 37 (2023) e5505, https://doi.org/10.1002/bmc.5505.
[22] F. Ma, S. Li, X. Gao, J. Zhou, X. Zhu, D. Wang, Y. Cai, F. Li, Q. Yang, X. Gu, W. Ge, H. Liu, X. Xiao, H. Hao, Interleukin-6-mediated CCR9+ interleukin-17-producing regulatory T cells polarization increases the severity of necrotizing enterocolitis, EBioMedicine 44 (2019) 71–85, https://doi.org/10.1016/j.ebiom.2019.05.042.
[23] M. Good, C.P. Sodhi, J.A. Ozolek, R.H. Buck, K.C. Goehring, D.L. Thomas, A. Vikram, K. Bibby, M.J. Morowitz, B. Firek, P. Lu, D.J. Hackam, Lactobacillus rhamnosus HN001 decreases the severity of necrotizing enterocolitis in neonatal mice and preterm piglets: evidence in mice for a role of TLR9, Am. J. Physiol. Gastrointest. Liver Physiol. 306 (2014) G1021–G1032, https://doi.org/10.1152/ajpgi.00452.2013.
[24] F. Ma, H. Hao, X. Gao, Y. Cai, J. Zhou, P. Liang, J. Lv, Q. He, C. Shi, D. Hu, B. Chen, L. Zhu, X. Xiao, S. Li, Melatonin ameliorates necrotizing enterocolitis by preventing Th17/Treg imbalance through activation of the AMPK/SIRT1 pathway, Theranostics 10 (2020) 7730–7746, https://doi.org/10.7150/thno.45862.
[25] T. Jilling, J. Lu, M. Jackson, M.S. Caplan, Intestinal epithelial apoptosis initiates gross bowel necrosis in an experimental rat model of neonatal necrotizing enterocolitis, Pediatr. Res. 55 (2004) 622–629, https://doi.org/10.1203/01.PDR.0000113463.70435.74.
[26] Y. Yin, B.-M. Tian, X. Li, Y.-C. Yu, D.-K. Deng, L.-J. Sun, H.-L. Qu, R.-X. Wu, X.-Y. Xu, H.-H. Sun, Y. An, X.-T. He, F.-M. Chen, Gold nanoparticles targeting the autophagy–lysosome system to combat the inflammation-compromised osteogenic potential of periodontal ligament stem cells: from mechanism to therapy, Biomaterials 288 (2022) 121743, https://doi.org/10.1016/j.biomaterials.2022.121743.
[27] K. Jung, I. Koh, J.-H. Kim, H.S. Cheong, T. Park, S.H. Nam, S.-M. Jung, C.A. Sio, S. Y. Kim, E. Jung, B. Lee, H.-R. Kim, E. Shin, S.-E. Jung, C.W. Choi, B.I. Kim, E. Jung, H.D. Shin, RNA-seq for gene expression profiling of human necrotizing enterocolitis: a pilot study, J. Kor. Med. Sci. 32 (2017) 817, https://doi.org/10.3346/jkms.2017.32.5.817.
[28] C. Liu, C. Fu, Y. Sun, Y. You, T. Wang, Y. Zhang, H. Xia, X. Wang, Itaconic acid regulation of TFEB-mediated autophagy flux alleviates hyperoxia-induced bronchopulmonary dysplasia, Redox Biol. 72 (2024) 103115, https://doi.org/10.1016/j.redox.2024.103115.
[29] A. Ballabio, J.S. Bonifacino, Lysosomes as dynamic regulators of cell and organismal homeostasis, Nat. Rev. Mol. Cell Biol. 21 (2020) 101–118, https://doi.org/10.1038/s41580-019-0185-4.
[30] X. Shi, H. Zhou, J. Wei, W. Mo, Q. Li, X. Lv, The signaling pathways and therapeutic potential of itaconate to alleviate inflammation and oxidative stress in inflammatory diseases, Redox Biol. 58 (2022) 102553, https://doi.org/10.1016/j.redox.2022.102553.
[31] M.D. Neal, C.P. Sodhi, M. Dyer, B.T. Craig, M. Good, H. Jia, I. Yazji, A. Afrazi, W. M. Richardson, D. Beer-Stolz, C. Ma, T. Prindle, Z. Grant, M.F. Branca, J. Ozolek, D. J. Hackam, A critical role for TLR4 induction of autophagy in the regulation of enterocyte migration and the pathogenesis of necrotizing enterocolitis, J. Immunol. 190 (2013) 3541–3551, https://doi.org/10.4049/jimmunol.1202264.
[32] C.L. Leaphart, J. Cavallo, S.C. Gribar, S. Cetin, J. Li, M.F. Branca, T.D. Dubowski, C. P. Sodhi, D.J. Hackam, A critical role for TLR4 in the pathogenesis of necrotizing enterocolitis by modulating intestinal injury and repair, J. Immunol. 179 (2007) 4808–4820, https://doi.org/10.4049/jimmunol.179.7.4808.
[33] R.-Q. Yao, C. Ren, Z.-F. Xia, Y.-M. Yao, Organelle-specific autophagy in inflammatory diseases: a potential therapeutic target underlying the quality control of multiple organelles, Autophagy 17 (2021) 385–401, https://doi.org/10.1080/15548627.2020.1725377.
[34] N. Mizushima, M. Komatsu, Autophagy: renovation of cells and tissues, Cell 147 (2011) 728–741, https://doi.org/10.1016/j.cell.2011.10.026.
[35] I. Tanida, N. Minematsu-Ikeguchi, T. Ueno, E. Kominami, Lysosomal turnover, but not a cellular level, of endogenous LC3 is a marker for autophagy, Autophagy 1 (2005) 84–91, https://doi.org/10.4161/auto.1.2.1697.
[36] C. Settembre, C. Di Malta, V.A. Polito, M.G. Arencibia, F. Vetrini, S. Erdin, S. U. Erdin, T. Huynh, D. Medina, P. Colella, M. Sardiello, D.C. Rubinsztein, A. Ballabio, TFEB links autophagy to lysosomal biogenesis, Science 332 (2011) 1429–1433, https://doi.org/10.1126/science.1204592.
[37] L. Li, M. Yu, Y. Li, Q. Li, H. Yang, M. Zheng, Y. Han, D. Lu, S. Lu, L. Gui, Synergistic anti-inflammatory and osteogenic n-HA/resveratrol/chitosan composite microspheres for osteoporotic bone regeneration, Bioact. Mater. 6 (2021) 1255–1266, https://doi.org/10.1016/j.bioactmat.2020.10.018.

[38] R.P. Wang, W. Leung, T. Goto, J.Y. Ho, R.C. Chang, IL-1 beta and TNF-alpha play an essential role in modulating the risk of both periodontitis and Alzheimer's disease, Alzheimers Dement 17 (2021) e058464, https://doi.org/10.1002/alz.058464.

[39] L. Yu, Y. Chen, S.A. Tooze, Autophagy pathway: cellular and molecular mechanisms, Autophagy 14 (2018) 207–215, https://doi.org/10.1080/15548627.2017.1378838.

[40] S.R. Bonam, F. Wang, S. Muller, Lysosomes as a therapeutic target, Nat. Rev. Drug Discov. 18 (2019) 923–948, https://doi.org/10.1038/s41573-019-0036-1.

[41] N.R. Komilova, P.R. Angelova, A.V. Berezhnov, O.A. Stelmashchuk, U. Z. Mirkhodjaev, H. Houlden, A.V. Gourine, N. Esteras, A.Y. Abramov, Metabolically induced intracellular pH changes activate mitophagy, autophagy, and cell protection in familial forms of Parkinson's disease, FEBS J. 289 (2022) 699–711, https://doi.org/10.1111/febs.16198.

[42] F. Michopoulos, N. Karagianni, N.M. Whalley, M.A. Firth, C. Nikolaou, I.D. Wilson, S.E. Critchlow, G. Kollias, G.A. Theodoridis, Targeted metabolic profiling of the Tg197 mouse model reveals itaconic acid as a marker of rheumatoid arthritis, J. Proteome Res. 15 (2016) 4579–4590, https://doi.org/10.1021/acs.jproteome.6b00654.

[43] K. Ren, Y. Lv, Y. Zhuo, C. Chen, H. Shi, L. Guo, G. Yang, Y. Hou, R.X. Tan, E. Li, Suppression of IRG-1 reduces inflammatory cell infiltration and lung injury in respiratory syncytial virus infection by reducing production of reactive oxygen species, J. Virol. 90 (2016) 7313–7322, https://doi.org/10.1128/JVI.00563-16.

[44] T. Cordes, A. Lucas, A.S. Divakaruni, A.N. Murphy, P. Cabrales, C.M. Metallo, Itaconate modulates tricarboxylic acid and redox metabolism to mitigate reperfusion injury, Mol. Metabol. 32 (2020) 122–135, https://doi.org/10.1016/j.molmet.2019.11.019.

[45] V.V. Loi, T. Busche, B. Kuropka, S. Müller, K. Methling, M. Lalk, J. Kalinowski, H. Antelmann, Staphylococcus aureus adapts to the immunometabolite itaconic acid by inducing acid and oxidative stress responses including S-bacillithiolations and S-itaconations, Free Radic. Biol. Med. 208 (2023) 859–876, https://doi.org/10.1016/j.freeradbiomed.2023.09.031.

[46] A.V. Berezhnov, M.P.M. Soutar, E.I. Fedotova, M.S. Frolova, H. Plun-Favreau, V. P. Zinchenko, A.Y. Abramov, Intracellular pH modulates autophagy and mitophagy, J. Biol. Chem. 291 (2016) 8701–8708, https://doi.org/10.1074/jbc.M115.691774.

[47] Z. Zhang, C. Chen, F. Yang, Y.-X. Zeng, P. Sun, P. Liu, X. Li, Itaconate is a lysosomal inducer that promotes antibacterial innate immunity, Mol. Cell. 82 (2022) 2844–2857.e10, https://doi.org/10.1016/j.molcel.2022.05.009.